Switching and charge-density-wave transport in $NbSe_3$. I. dc characteristics

R. P. Hall,* M. F. Hundley, and A. Zettl
Department of Physics, University of California, Berkeley, California 94720
(Received 11 January 1988)

The phenomenon of switching is studied in the lower charge-density-wave (CDW) state of $NbSe_3$ by measurements of dc conductivity. Results show that switching is distinguished from nonswitching CDW transport by discontinuities in CDW current, large polarization before the onset of CDW motion, and an unusual temperature dependence of the electric fields necessary to initiate CDW motion. Furthermore, switching behavior is found to originate within the crystalline bulk of $NbSe_3$. Switching is not caused by surface defects or external electrical contacts, but is instead produced by strong, nonuniform pinning of a CDW. Standard models of CDW transport cannot explain the experimental results. In particular such models neglect fluctuations of the CDW amplitude, but the observation of current discontinuities indicates that amplitude fluctuations occur within switching crystals. We suggest that amplitude fluctuations, caused by order-parameter oscillations at phase-slip centers, produce a breakdown in pinning that leads to switching behavior. We discuss the possible origin of phase-slip centers in $NbSe_3$, and define two length scales that, in conjunction with the Fukuyama-Lee-Rice phase coherence length, set a criterion for the occurrence of switching.

I. INTRODUCTION

Charge-density-wave (CDW) transport has been observed in a variety of quasi-one-dimensional conductors.[1] These conductors are typically anisotropic metals at room temperature but undergo a phase transition into the Peierls distorted state at lower temperatures. Following a Peierls transition, a gap opens up at the electronic Fermi surface as the crystal lattice and electronic charge density $\rho(x)$ become spatially modulated:

$$\rho(x)=\bar{\rho}+\rho_{\mathrm{CDW}}\cos(Qx+\phi)\ . \tag{1}$$

Here $\bar{\rho}$ is the average electronic density, ρ_{CDW} is the amplitude of the electronic density wave, $Q=2k_F$ is the CDW wave vector, with k_F the electronic Fermi wave vector, and ϕ is the CDW phase with respect to the undistorted lattice. If the CDW wave length $\lambda=2\pi/Q$ is incommensurable with the lattice constant a, then in an ideal crystal the energy of a CDW would be independent of its phase. Therefore the application of an electric field, even a vanishingly small electric field, would cause the CDW to slide and carry an electrical current.

Because impurities and defects pin the CDW phase to preferred local values, the energy of a CDW in a real (i.e. nonideal) crystal is not independent of the CDW phase.[2-5] If the impurity and defect concentrations are small enough, however, an electric field E can still depin a CDW, leading to a sliding CDW state with enhanced conductivity. In conventional CDW depinning, the depinning process is smooth, with a well-defined threshold field E_T for the onset of CDW conduction and with no discontinuities in either chordal (V/I) or differential (dV/dI) resistance.[6] At very high electric fields the CDW dynamic conductance saturates as the CDW approaches a high-field, high-conductivity state.[6-8]

In contrast to conventional CDW depinning, the phenomenon of switching produces a sharp, often hysteretic discontinuity in the I-V characteristic of a CDW conductor.[9] In many cases, the critical field E_c at which switching occurs corresponds to the onset of CDW motion, hence $E_c=E_T$. In other cases, switching is preceded by apparently conventional CDW depinning, so $E_c>E_T$.[10] Multiple switches in a single I-V characteristic have also been reported.[11] Switching may be observed in real-time pulsed experiments, where application of a current pulse causes an abrupt transition to a high-conductivity state after a short delay time.[9,12] Switching was first reported in the lower CDW state of $NbSe_3$. Since then, switching has been observed in selected crystals of TaS_3,[13] $(NbSe_4)_{3.33}I$,[14] $K_{0.3}MoO_3$, nd $Rb_{0.3}MoO_3$.[15] Furthermore, switching has been intentionally induced or enhanced by iron doping $NbSe_3$ (Ref. 11) or by irradiating the blue bronzes.[16] Therefore, switching has proven to be a rather general CDW phenomena.

The magnitude of switching thresholds is characteristic of CDW depinning energies and suggests that the non-Ohmic current in switching crystals is carried by the CDW condensate, just as in nonswitching crystals. On the other hand, CDW transport is dramatically different in switching crystals than in nonswitching crystals. For example, switching in $NbSe_3$ is associated with hysteresis,[9] negative differential resistance,[17] bistability and large $1/f$ noise,[17] an inductive ac response,[18] and period-doubling routes to chaos.[19] In nonswitching $NbSe_3$ crystals, all of these effects are absent. Most experimental and theoretical research has concentrated on smoothly depinning CDW's in nonswitching crystals. A number of models, both quantum[20] and classical,[21,22] have partially explained the dynamics of this type of CDW. Despite a wide diversity of physical assumptions, these standard models commonly ascribe CDW motion to variations in

the CDW phase and treat the CDW amplitude as constant and homogeneous throughout a crystal.

Because of the drastic differences between switching and nonswitching crystals, various *ad hoc* mechanisms have been introduced to explain switching: domain coupling,[9,23] CDW self-blocking,[24] CDW inertia,[19] and CDW current noise.[25] *Ad hoc* explanations for switching are rather unsatisfactory, in the sense that they tend to obscure a fundamental issue. Because it is unclear whether quantum tunneling or classical mechanics is the appropriate framework for describing CDW dynamics in general, the physical nature of CDW transport remains controversial. However, switching could provide a stringent test for any general theory of CDW dynamics. A theoretical model which correctly describes conventional CDW dynamics should be a limiting case of a more general description which encompasses switching. Thus it is important to understand switching at a fundamental level.

This paper, along with several companion papers,[26–28] presents the results of a study on switching in $NbSe_3$. The primary goal of this study was to determine whether switching is an intrinsic aspect of CDW transport. The results of this study show that it indeed is. More precise goals of this study were to characterize the dynamics of switching CDW's, to relate these dynamics to the dynamics of nonswitching CDW's, and to compare the dynamics of switching CDW's to the predictions of existing models. The main conclusion of our research is that switching corresponds to a new regime of CDW dynamics: CDW motion in the presence of strong, nonuniform pinning. (We clarify what is meant by "nonuniform" in the analysis of our results.) Phase slippage and amplitude fluctuations are basic features of the transport of switching CDW's. As a result, switching cannot be adequately described by any purely phase-dynamical model of CDW sliding—a dynamical treatment of the CDW amplitude is also required. Although we have limited our study to a single CDW material, we believe that our results are applicable to the other CDW conductors as well.

In this paper, we discuss the response of switching crystals of pure and iron-doped $NbSe_3$ to applied dc fields. Experimental methods include measurement of I-V and dV/dI characteristics, and of narrow-band noise. Also reported are the results of temperature-gradient experiments and spatially resolved measurements. The paper and results are organized as follows. In Sec. II, on materials and methods, we discuss factors that influence the occurrence of switching in $NbSe_3$ crystals. In Sec. III we report measurements of dc CDW conductivity. The measurements fall into three groups: characterization of dc properties, study of their temperature dependence, and examination of their spatial uniformity within single switching crystals. In Sec. IV we summarize and then analyze the experimental results. In Sec. V, the Conclusion, we discuss the relevance of our findings to other aspects of CDW transport.

II. MATERIALS AND METHODS

Samples used in our experiments consisted of single crystals of nominally pure and iron-doped $NbSe_3$, prepared by conventional vapor-transport methods.[8] The amount of iron incorporated into the Fe_xNbSe_3 crystals ($x=0.03$ by starting materials) was much less than the nominal doping, below the approximately 1% sensitivity of a microprobe analysis. Precisely where in the $NbSe_3$ matrix the iron was incorporated (substitutionally or between the chains) was not determined. Typical crystal dimensions for both the Fe_xNbSe_3 and $NbSe_3$ crystals were $2\ \text{mm}\times 3\ \mu\text{m}\times 2\ \mu\text{m}$.

Crystals of nominally pure $NbSe_3$ were obtained from several different preparation lots, each produced by identical procedures. Switching was observed only in the lower CDW state, but was not extensively searched for in the upper CDW state. The ratio of switching to nonswitching samples varied widely among $NbSe_3$ batches. In some lots, no samples displayed switching, whereas in others over 50% of the samples showed switching. The incidence of switching was found to depend on the age of a batch. In particular, crystals over six months old did not display switching. Nearly the original incidence of switching could be restored, however, by etching the batch in hot, concentrated H_2SO_4. A similar aging effect was observed in Fe_xNbSe_3, but etches of H_2SO_4 were less effective in restoring switching in this material. The incidence of switching was consistently higher in Fe_xNbSe_3 than in $NbSe_3$.

We studied the incidence of switching as a function of sample dimension and quality. Sample quality was monitored either by the number of surface defects, measured by scanning electron microscopy, or by crystal purity, measured by either the threshold field at 48 K or by the residual resistivity ratio. No dependence was observed on either sample dimension or quality. Preliminary results had shown switching to be more prevalent in thinner samples,[10] but simply reducing a given sample's cross section did not consistently induce switching. For example, reducing the cross section of a well-aged crystal had no effect on its I-V characteristic. A correlation of switching with cross-sectional area does exist, but it is related to the issue of transverse CDW coherence, as is discussed later in this paper.

Current leads were applied to crystals using silver paint and fine gold wires. Both two-probe and four-probe conductivity measurements were made. For the four-probe measurements, a special sample holder was constructed that enabled voltages to be measured anywhere along a sample's length;[29] this probe is described in Sec. II. Conductivity measurements were also made when temperature gradients were applied across the samples. For these measurements, crystals were suspended in vacuum between two large copper mounting posts that were thermally anchored to Peltier heater chips. Thermometry was accomplished through a diode sensor and several differential thermocouples mounted close to the samples.

III. RESULTS

A. I-V characteristics and threshold fields

Switching I-V characteristics of pure and iron-doped $NbSe_3$ crystals were found to be nearly identical. Figure

1(a) shows current-driven I-V characteristics that are typical for switching crystals of $NbSe_3$, at selected temperatures in the lower CDW state. Figure 1(b) shows similar I-V characteristics for Fe_xNbSe_3. Switching occurs only over a limited temperature range, from about

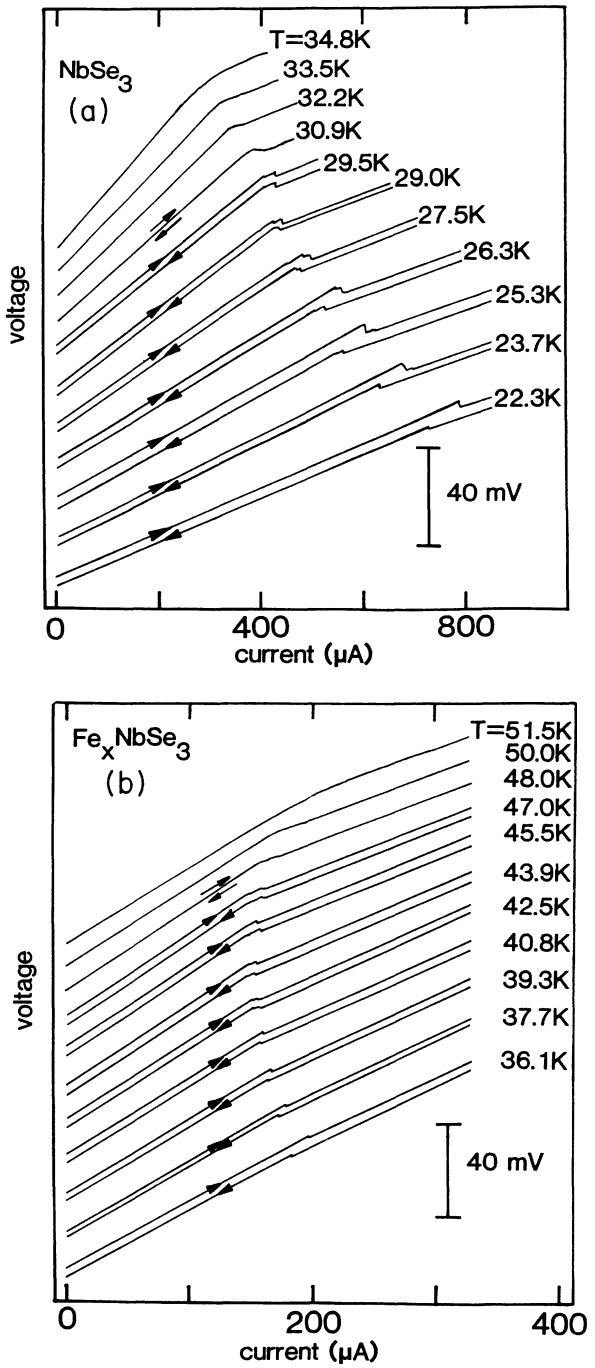

FIG. 1. (a) Current-driven dc I-V curves for a switching crystal of $NbSe_3$. Arrows indicate the direction of bias sweep. For temperatures below 30 K, the traces for forward- and reverse-bias sweeps have been vertically offset for clarity. (b) Current-driven dc I-V curves for a switching crystal of Fe_xNbSe_3. Arrows indicate the direction of bias sweep. For temperatures below 48 K, the traces for forward- and reverse-bias sweeps have been vertically offset for clarity.

15 to 35 K in $NbSe_3$ and from about 40 to 50 K in Fe_xNbSe_3. These temperature ranges are somewhat sample dependent. In $NbSe_3$, for example, switching may occur at temperatures as high as 42 K, or it may not begin until below 30 K. In both $NbSe_3$ and Fe_xNbSe_3, at temperatures above the switching regime, the chordal resistance V/I is a smooth function of the applied current bias, and the differential resistance dV/dI remains positive along the I-V curve. As the switching regime is entered, a region of negative differential resistance appears and develops into an abrupt switch with decreasing temperature. Well into the switching regime, switching becomes hysteretic, and departure from the switching regime occurs at lower temperatures, as the switch height decreases and hysteresis increases. Multiple as well as single switches are observed in Fe_xNbSe_3 and $NbSe_3$, and switching occurs in either voltage or current-driven experiments. [As an example, Fig. 6(b) shows a voltage-driven I-V characteristic of a $NbSe_3$ crystal with nine switches.] The size of switching is sample dependent. The largest switching, i.e., the largest relative discontinuity in an I-V characteristic, was observed in undoped $NbSe_3$ crystals.

A feature common to both $NbSe_3$ and Fe_xNbSe_3 is that dynamic conductance is roughly constant past the switching threshold.[10] This may be seen in the I-V curves of Fig. 1, where the switching curves have nearly uniform slope in the nonlinear region. In *non*switching crystals, the inverse differential conductance dV/dI attains constant values only when the applied field is about 4–5 times the threshold field.[6] Switching crystals reach the high-field conductivity state immediately past threshold, which suggests that CDW pinning effectively collapses at threshold.

The critical threshold field E_c in switching crystals is nearly independent of temperature. The temperature independence of switching thresholds in $NbSe_3$ crystals is quite striking. Figure 2(a) shows threshold fields of switching and nonswitching $NbSe_3$ crystals, normalized to their extrapolated $T=0$ values. (Normalization is necessary because of the wide spread in threshold fields; see below.) For reference, the figure also displays Fleming's curve for threshold fields in nonswitching $NbSe_3$ crystals.[6] Threshold fields E_T have the same general temperature dependence for all nonswitching samples; e.g., they begin to rise gradually as the temperature is cooled below 50 K and change by about 100% between 35 and 20 K. In contrast, E_T in switching samples rises quite abruptly just before the switching regime is entered, and then is roughly constant, to within 10%, inside the switching regime where $E_T=E_c$. In the temperature range 41–46 K, half-filled symbols indicate switching thresholds E_c that are preceded by conventional depinning, with $E_T<E_c$.

The temperature independence of switching thresholds in Fe_xNbSe_3 is somewhat less dramatic, because nonswitching thresholds are less temperature dependent between 40 and 50 K. Figure 2(b) shows threshold fields of a switching Fe_xNbSe_3 crystal and a nonswitching $NbSe_3$ crystal. The threshold fields have been arbitrarily

normalized to their 51-K values, and again for reference the figure displays Fleming's curve for nonswitching $NbSe_3$ threshold fields. Switching in this Fe_xNbSe_3 crystal occurred mainly between 40 and 48 K. In this temperature range, the crystal's threshold field $E_T=E_c$ is nearly constant (solid circles). In contrast, threshold fields of nonswitching crystals change by 50% between these temperatures. Outside of the switching regime, the threshold field E_T of the Fe_xNbSe_3 crystal is strongly temperature dependent (open circles). The atypical temperature dependence of switching thresholds—in $NbSe_3$ and Fe_xNbSe_3—suggests that a different physical mechanism is responsible for CDW depinning in switching crystals than the usual phase depinning that occurs in nonswitching crystals.[10]

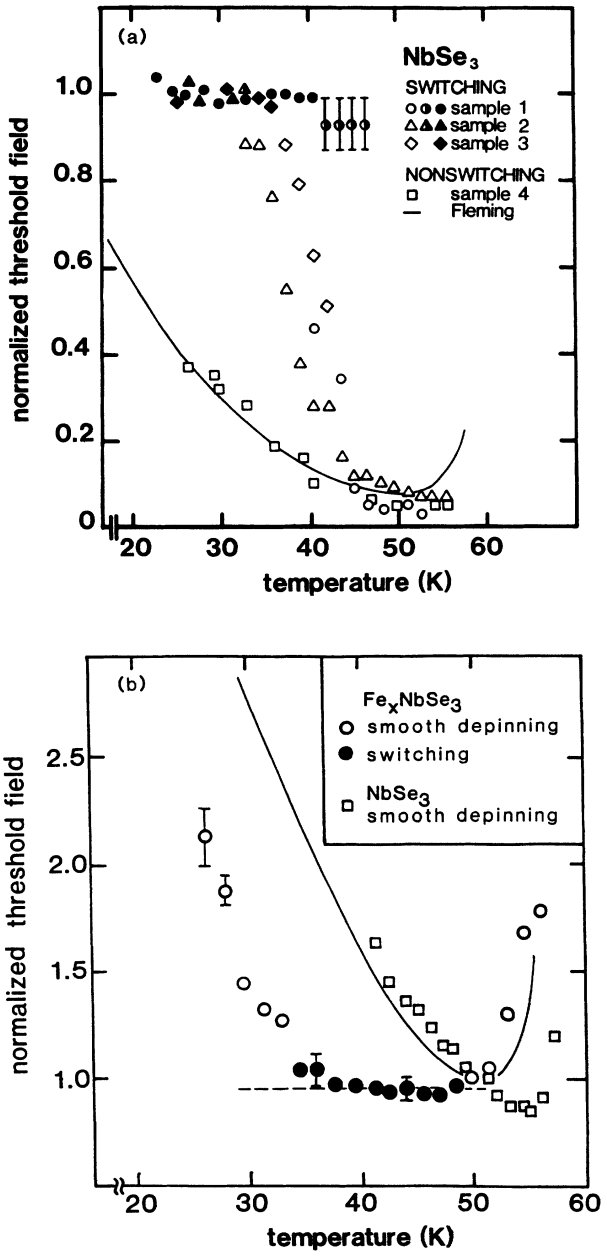

FIG. 2. (a) Normalized threshold fields for CDW depinning in switching and nonswitching crystals of $NbSe_3$. The open symbols represent thresholds E_T for smooth depinning, the solid symbols represent thresholds $E_c=E_T$ for switching, and the half-filled symbols represent switching thresholds E_c when a crystal depins smoothly at a lower bias E_T. Fleming's curve for nonswitching thresholds is adapted from Ref. 6. (b) Normalized threshold fields for a switching Fe_xNbSe_3 crystal and a nonswitching $NbSe_3$ crystal. Fleming's curve for nonswitching $NbSe_3$ is adapted from Ref. 6.

Switching threshold fields E_c are generally large, and in the switching regime the onset of nonlinear conduction typically occurs at $E_T=E_c$. In $NbSe_3$, switching thresholds are between 300 and 1500 mV/cm, and in Fe_xNbSe_3, switching thresholds are between 100 and 500 mV/cm. These fields are 10–100 times larger than nonswitching thresholds observed at comparable temperatures in the highest-quality $NbSe_3$ crystals.[6,30] Although switching fields are always large, nonswitching thresholds can be equally large, and comparisons of threshold fields in randomly selected crystals reveal no critical value of threshold field above which switching always occurs.

A more fruitful comparison is of E_c for switching and E_T for nonswitching behavior in the *same* crystal. Other researchers have performed this kind of comparison by irradiating nonswitching crystals.[16] They find that irradiation produces switching, and that the onset of switching is accompanied by an increase in threshold field E_T. We have performed the inverse experiment: we have induced nonswitching behavior in switching crystals. By physically cutting and thereby shortening a switching crystal, switching can be eventually eliminated. Figure 3 shows $J=I/A$ (A denotes the sample cross-sectional area) versus E curves for a $NbSe_3$ crystal at 35 K. The uncut crystal was 2.8 mm long and displayed a large hysteretic switch at a threshold field of $E_1=1450$ mV/cm. The cut crystal was 300 μm shorter, and depinned smoothly at $E_2=480$ mV/cm. (No additional nonlinearity was observed at 1450 mV/cm.) Other crystals displayed the same general dependence of switching on length, al-

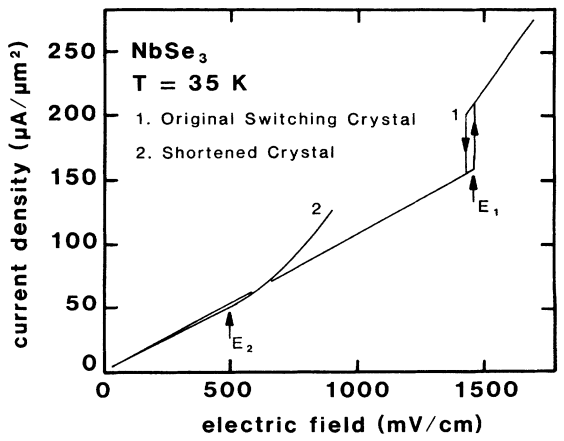

FIG. 3. Voltage-driven, switching I-V curve for an unit crystal of $NbSe_3$, and nonswitching I-V curve for the same crystal after it has been shortened from 2.8 to 2.5 mm.

though not as dramatically; some crystals were shortened to 100 μm before they stopped switching.

B. Nonuniform pinning

Reducing the length of a *non*switching crystal does not induce switching, but reducing the cross-sectional area sometimes does. $NbSe_3$ crystals may be easily cleaved by splitting them parallel to the *b-c* or *b-a* planes of the unit cell. Figure 4 shows a micrograph of a crystal that was split from a larger crystal. The length of both split and unsplit crystals was 2.5 mm. The cross-sectional area of the unsplit crystal was 28 μm^2, whereas the cross-sectional area of the split crystal was 2.7 μm^2. The split crystal appears uniform, with no damage visible anywhere along the crystal surface, indicating that splitting is an effective way of reducing a crystal's cross-sectional area in a nondestructive way.

Figures 5(a) and 5(b) show *J-E* curves at 29 K for the parent crystal and for the split crystal of Fig. 4, respectively. The parent crystal depins smoothly at $E_T=48$ mV/cm, but the split crystal switches at $E_c=E_T=675$ mV/cm. Threshold fields at 48 K, a standard measure of crystal quality, also changed. The threshold field of the starting crystal was 16 mV/cm, but the threshold field of the split crystal was 70 mV/cm. The higher threshold fields of the split crystal—both at 48 and 29 K—indicate that the CDW is pinned more effectively in the split (switching) than in the unsplit (nonswitching) crystal.

Similar changes in switching and threshold field were observed in a number of other split crystals. The effect of splitting suggests the presence of localized, strongly pinning regions, sparsely distributed within $NbSe_3$ and Fe_xNbSe_3 crystals. Elimination of these strongly pinning regions (as occurs by physically cutting them from the crystal) causes a switching crystal to become nonswitching. Conversely, reducing the cross-sectional area of a crystal by splitting may induce switching in a previously nonswitching crystal. If the width of a crystal is large compared to the CDW phase-coherence length, then CDW current can flow around localized regions that are strongly pinned, leading to uniform depinning with no switching. On the other hand, if the crystal width is comparable to the transverse coherence length, then localized regions of strong pinning can initially obstruct CDW current and ultimately result in switching. Transverse phase-coherence lengths in $NbSe_3$ are roughly 0.4–0.8 μm for threshold fields of 16–70 mV/cm.[31] Therefore the diameter of the split crystal in Fig. 4 is comparable to the transverse CDW coherence length. In contrast, the diameter of the unsplit crystal is much larger, which is consistent with the much smaller pinning in that crystal.

We now turn to another series of experiments, where current domains were directly observed by nonperturbative measurements of local dc conductivities.[29] Figure 6(a) schematically illustrates the four-terminal probe used to make such measurements. Current leads, terminals 1 and 4, were attached to the ends of a crystal using silver

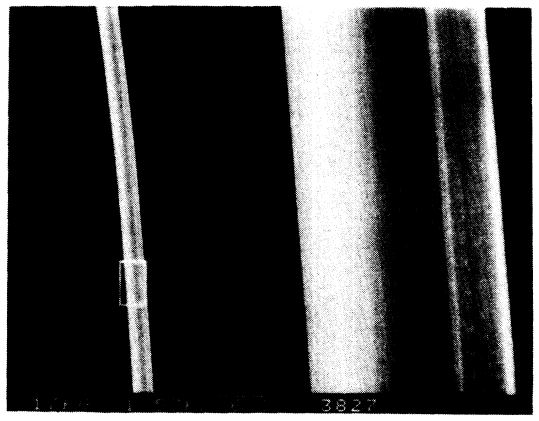

FIG. 4. Scanning-electron-microscopy micrograph of a switching $NbSe_3$ crystal. No surface defects are apparent. Left: typical crystal section. Right: detail of boxed region on the left, magnification by an additional factor of 10. Scale bar of 6.37 μm refers to the left-hand photo.

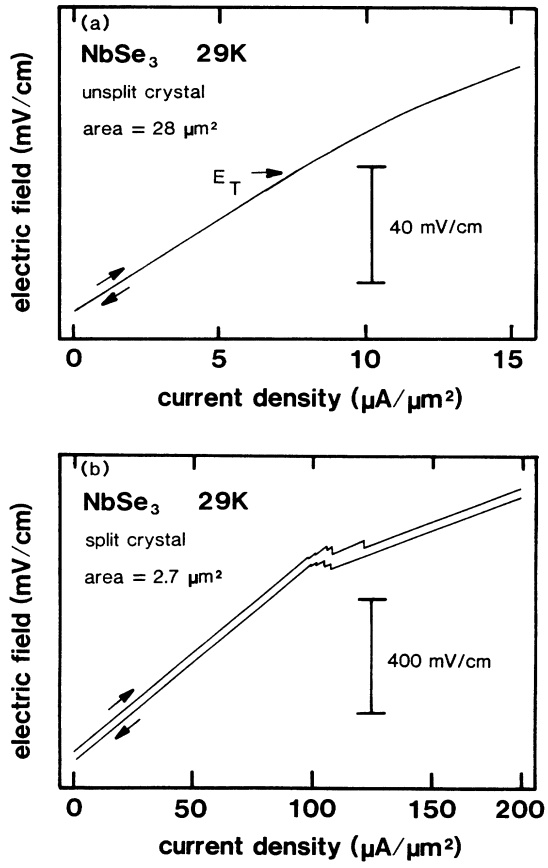

FIG. 5. (a) Current-driven *I-V* characteristics of a $NbSe_3$ crystal at $T=29$ K. The traces of forward- and reverse-bias sweeps have been offset vertically for clarity. The threshold field E_T is indicated by an arrow for the lower trace. (b) Current-driven *I-V* characteristics for a $NbSe_3$ crystal at $T=29$ K. The crystal was obtained by "splitting" the parent crystal of (a). Multiple switching is clearly observed. The traces for forward- and reverse-bias sweeps have been vertically offset for clarity.

paint. Two additional voltage-sensing leads, terminals 2 and 3, were formed by pressing fine metal wires against the crystal surface. The pressures as well as locations of probes 2 and 3 could be adjusted independently during an experiment. Adjusting the pressure of the probes changed their contact resistance to the crystal. When the probes were lightly applied, their contact resistances were large and the probes did not perturb the current distributions within a crystal. The probes could be placed anywhere along a crystal with an accuracy of ± 5 μm.

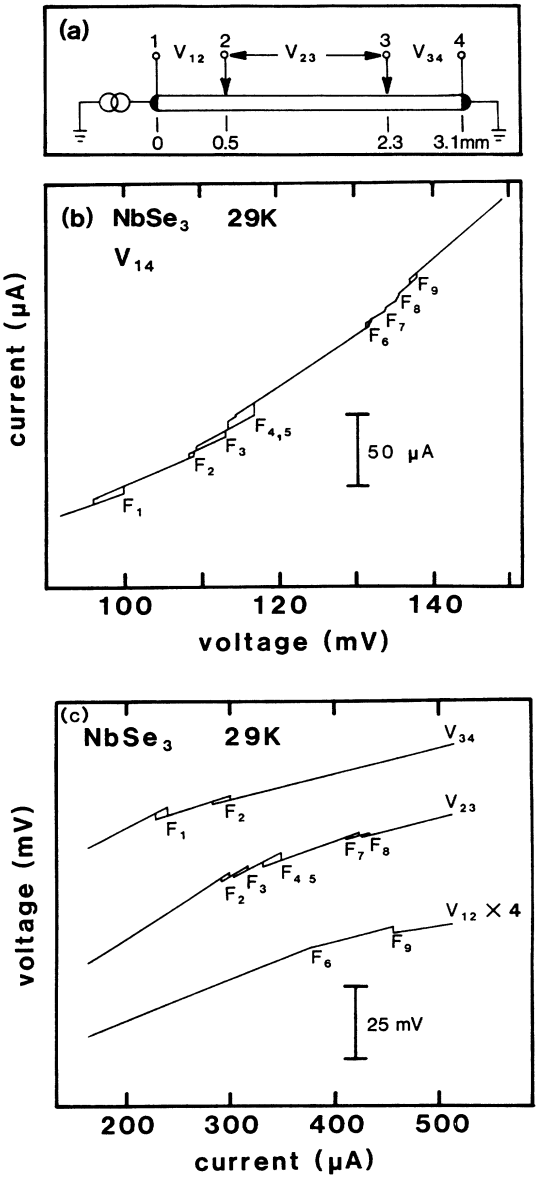

FIG. 6. (a) Four-terminal measurement configuration. Terminals 2 and 3 are movable and nonperturbative. The indicated distances refer to terminal positions used in (b) and (c). (b) Voltage-driven I-V characteristics of a $NbSe_3$ crystal at $T=29$ K, measured between terminals 1 and 4 (2 probe) as indicated in (a). The traces for forward- and reverse-bias sweeps have been offset vertically for clarity. The switches are identified with a number, which also identifies a particular peak in the narrow-band noise spectrum (see Fig. 7). (c) Current-driven I-V characteristics for the same $NbSe_3$ crystal as used in (b). The three traces refer to the local I-V characteristic of three different segments of the crystal [see (a)].

Figure 6(b) displays a voltage-driven I-V characteristic of a $NbSe_3$ crystal with nine switches, measured across terminals 1 and 4. The switches were unaffected by either contact 2 or 3, whether the contacts were lifted or applied. Figure 6(c) shows current-driven I-V characteristics across successive segments of the same crystal, when probes 2 and 3 were lightly applied to the crystal. (Segment lengths are shown in the inset.) Figure 6(c) shows that when a switch occurs in a complete I-V characteristic a corresponding switch occurs in at least one, but not all, of the partial I-V characteristics. Therefore, each switch signals local depinning of the CDW. Threshold fields vary by 50% in Fig. 6(c), so the CDW is nonuniformly pinned within the crystal.

We find that switching in $NbSe_3$ and Fe_xNbSe_3 is generally characterized by nonuniform pinning and formation of current domains. Narrow-band noise measurements show that the CDW drift velocity within a current domain is independent of its drift velocity within other domains.[29] For example, each successive switch in Fig. 6(b) corresponds to a new fundamental noise frequency entering the total noise spectrum. Figure 7 shows traces of frequency versus total CDW current for the first six narrow-band noise fundamentals. Unlike nonswitching crystals, the frequency of a fundamental is not proportional to the *total* excess CDW current. Each switch produces a jump in the total CDW current and thus a break in the traces of Fig. 7. After each switch, the slope of each frequency trace is lower, as would be expected if CDW current was to flow in spatially separated domains.

The size of a current-carrying domain may be estimat-

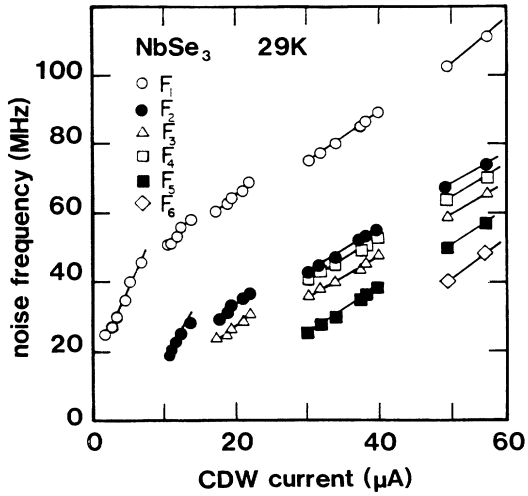

FIG. 7. Narrow-band noise frequency *total* CDW current for the same $NbSe_3$ crystal as used in Figs. 6(b) and 6(c). The measurement is performed between terminals 1 and 4 (2 probe). The different symbols refer to noise peaks which first appear at a particular switch, and are associated with a specific current domain. The data become linear and extrapolate to (0,0) only if the excess current axis is that appropriate to the specific current-carrying domain.

ed from $J'_{CDW} = ne\lambda f'$, where J'_{CDW} is the excess current density carried by that particular domain, n is the density of carriers condensed in the CDW state, λ is the CDW wavelength, and f' is the frequency generated by that domain. For example, assuming that $n = 10^{21}$ cm^{-3} and $\lambda = 14$ Å, the first switch in Fig. 6(a) corresponds to a volume of 2100 μm^3, which agrees with the crystal dimensions and the probe spacing. This volume indicates a serial arrangement of domains, i.e., domains stacked end to end along the crystal rather than side by side across the crystal. The slope of frequency versus current in Fig. 7 also indicates a serial arrangement of domains within the crystal.

The volume and arrangement of current domains may be determined directly by moving probes 2 and 3 independently along a crystal and measuring I-V characteristics in different sample segments.[29] We have performed such measurements in a number of $NbSe_3$ and Fe_xNbSe_3 crystals. Figure 8(a) shows the probe arrangement and Fig. 8(b) shows the I-V characteristics for a single Fe_xNbSe_3 crystal. The solid I-V curve (between terminals 1 and 4) indicates two distinct switches. By independently moving probes 2 and 3 and remeasuring the I-V characteristics, we determined that the first switch at I_{S1} corresponds to the depinning of a region A, whereas the second switch at I_{S2} corresponds to the depinning of a second region B. The two regions are identified at the top of the figure. The interface between regions A and B is very sharp. Figure 9(b) shows the magnitude of the switch at I_{S1} and the magnitude of the switch at I_{S2}, measured as functions of the positions of probes 2 and 3, respectively. The intersection of the lines through the data points indicates that the interface between regions A and B is well defined, and located 776 μm from terminal 1. Figures 8(a) and 8(b) are characteristic of switching samples of $NbSe_3$ and Fe_xNbSe_3. We consistently find that current domains are arranged serially and that interfaces between domains are abrupt to within the resolution of our probe (several micrometers). In these interface regions, CDW current is discontinuous. Condensed electrons are converted into normal carriers, and vice versa. Just as in superconductors[32] and superfluids,[33] current conversion takes place by periodic collapse of the CDW amplitude, at a rate set by the difference in CDW phase velocity between adjacent regions. These interface regions are therefore referred to as phase-slip centers.[29,34]

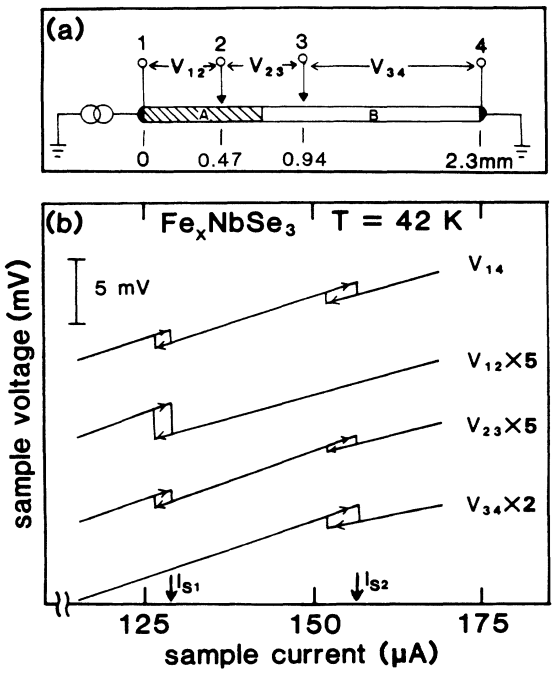

FIG. 8. (a) Voltage probe configuration for I-V traces shown in (b). (b) Simultaneously recorded current driven I-V traces for different segments of a single Fe_xNbSe_3 crystal at $T = 42$ K. I_{S1} and I_{S2} identify the two critical currents for switching.

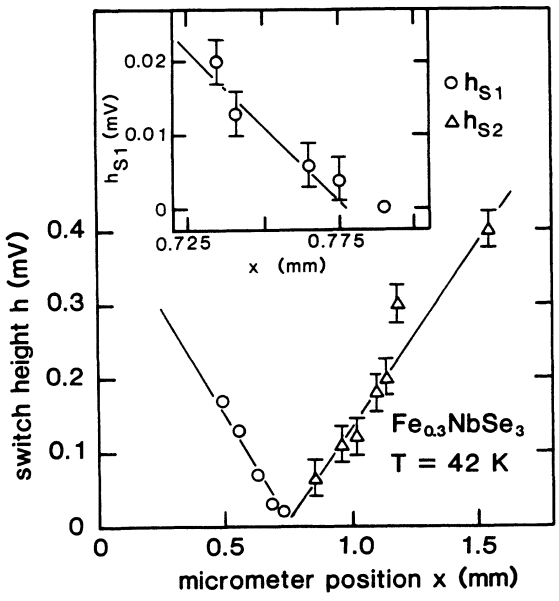

FIG. 9. Switching height h [as measured directly from I-V traces, such as shown in Fig. 8(b)], vs probe position for an Fe_xNbSe_3 crystal at $T = 42$ K. The circles refer to switch 1, the triangles refer to switch 2. The vertex of the two straight lines identifies the location of the phase-slip interface in this crystal. The inset shows h_{S1} near the phase-slip region in greater detail.

No distinguishing surface defects are associated with phase-slip centers. A scanning electron microscope was used to study the phase-slip region in the Fe_xNbSe_3 crystal of Figs. 8(a) and 8(b). Although some minor surface defects were evident, no major surface features were found in the phase-slip region. Conversely, some switching crystals, such as in Fig. 4, have virtually perfect surfaces. Switching thus cannot be ascribed to surface contamination or to surface defects.

C. Temperature-gradient experiments

We have demonstrated that pinning is nonuniform within switching crystals: switching crystals consist of a number of macroscopic current domains with independent threshold fields. A related issue is whether pinning is uniform inside one of these domains. Previous experiments, on crystals that display a large degree of switch-

ing, have demonstrated the development of sublevels within hysteresis loops as the temperature of the crystals is reduced.[35] The development of sublevels suggests that large current domains are susceptible to breakup into smaller domains, and that pinning therefore can be nonuniform within a single large domain. In crystals that display a small degree of switching, however, domains often show no tendency toward breakup and pinning could therefore be uniform within small regions. The domains associated with such regions appear "rigid."

To test the rigidity of apparently homogeneous domains, we applied temperature gradients across crystals that displayed a small degree of switching. In nonswitching $NbSe_3$, both the Ohmic resistivity and threshold field E_T are highly temperature dependent. An applied temperature gradient causes nonswitching crystals of $NbSe_3$ to break up into distinct current-carrying regions. Breakup is limited by the elasticity of the CDW phase and amplitude, which acts to keep the CDW drift velocity uniform even in the presence of effectively nonuniform pinning. Temperature gradients of 12–15 K/mm typically cause a nonswitching crystal to break into two or three well-defined regions.[36]

Although the critical threshold field for the onset of switching is temperature independent, the threshold current is not. This is a direct result of the strong temperature dependence of the Ohmic sample resistance in the switching regime. Figure 10(a) displays the I-V characteristics of a switching $NbSe_3$ crystal measured at selected temperatures. The entire crystal is at a uniform temperature in each case. The crystal shows negative differential resistance at 29 K and clear switching below 26 K. Below 26 K, depinning proceeds by two independent switches, labeled S_1 and S_2 in the figure, indicating that at least two current-carrying domains exist within the crystal. The two switches become hysteretic at low temperatures, but no additional switches are observed.

Figure 10(b) shows the effect of a temperature gradient across the same switching crystal of Fig. 10(a). One end of the crystal was held at a fixed temperature $T_0=24$ K, while the other end was warmed to a higher temperature $T_0+\Delta T$, between 24 and 28 K. The curves in Fig. 10(b) are labeled by the temperature difference ΔT. The length of the sample was 0.3 mm, and the largest gradient applied was 13 K/mm (for $\Delta T=4$ K). Figure 10(b) demonstrates that temperature gradients have a strong effect on the switching characteristics of $NbSe_3$. As the temperature gradient is increased, the first large switch [labeled S_1 in the top half of Fig. 10(b)] appears to break up into a series of smaller switches, labeled S_1', S_1'', etc. The second original switch, S_2, remains largely unaffected by the temperature gradient.

We associate the breakup of the original switch S_1 in Fig. 10(b) with a breakup of a switching domain near the warmer region of the crystal. The initial switch S_1' appears to correspond to a small domain very close to the warm end of the crystal. This is demonstrated in Fig. 11, which shows the threshold current of switch S_1' as a function of temperature (assuming $T=T_0+\Delta T$), along with the temperature dependence of S_1 (in the isothermal crystal) deduced from Fig. 10(a). The two thresholds match closely over the temperature range 24–28 K.

The results of Fig. 10(b) indicate that a temperature gradient as small as 6 K/mm is sufficient to break a current domain into four subdomains over a distance

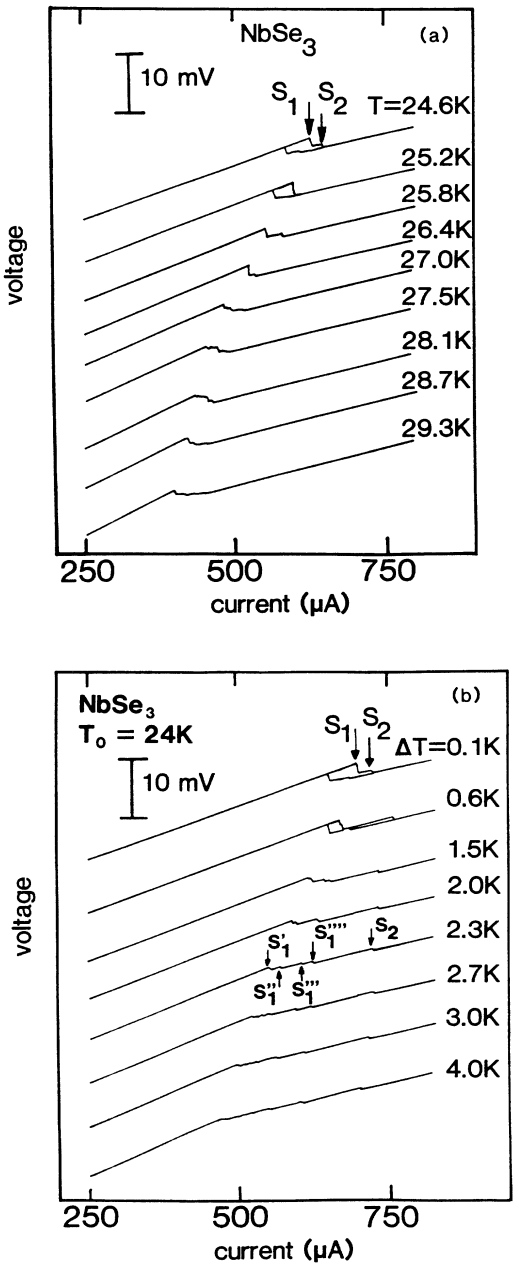

FIG. 10. (a) Current-driven I-V characteristics for a $NbSe_3$ crystal at selected temperatures. For each trace, the sample is isothermal. At low temperatures, two distinct switches, S_1 and S_2, occur as identified by the vertical arrows. (b) Current-driven I-V characteristics for the same $NbSe_3$ crystal as used in (a), but with a uniform temperature gradient applied. The cold end of the sample is held at $T_0=24$ K, the hot end is at $T_0+\Delta T$. With increasing ΔT, switch S_1 breaks up into a series of smaller switches, S_1', S_1'', etc., as identified in the $\Delta T=2.3$ K trace.

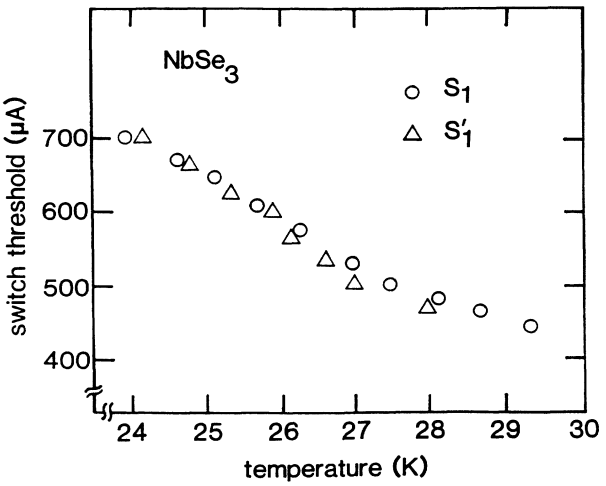

FIG. 11. Threshold current I_T vs temperature T for switching to occur in the same $NbSe_3$ crystal as used in Figs. 10(a) and 10(b). The open circles refer to switch S_1 of Fig. 10(a) (isothermal condition). The triangles refer to the first switch, S_1' of traces in Fig. 10(b) (gradient applied). The temperature used is $T_0+\Delta T$. The close correspondence of the two data sets indicate that S_1' is associated with a current domain near the warm end of the sample.

smaller than 300 μm. This distance is much smaller than the length typically associated with temperature-gradient-induced domains in nonswitching samples. The relatively large effect of a temperature gradient in switching samples indicates that pinning is nonuniform within the domain. The domain evidently consists of a number of coupled subregions, with an average length of less than 60 μm, that normally depin simultaneously (perhaps in an avalanche-type process). We propose that these subregions are actually separated by phase-slip centers, which cause velocity discontinuities only in the presence of an additional strain such as a temperature gradient. In a nonswitching crystal, the absence of phase-slip centers allows larger velocity-coherent domains in the presence of a temperature gradient.

D. CDW polarization

Local variations in threshold field should produce macroscopic polarization of the CDW in a switching crystal.[24] When an electric field exceeds the local threshold field, the CDW attempts to slide. If an adjacent region is not depinned, the elasticity of the CDW prevents CDW current from flowing until a phase-slip center forms or until the adjacent region depins. Phase-slip centers are energetically costly (see below), so the CDW phase can develop appreciable gradients across distances comparable to the Fukuyama-Lee-Rice phase-coherence length. Phase polarization is thought to be observed by localized resistivity changes in switching TaS_3 crystals.[12]

We have observed large, subthreshold resistivity changes in a switching $NbSe_3$ crystal by employing spatially resolved three-terminal dV/dI measurements. Figure 12(a) shows the contact arrangement. (The crystal regions A and B are meaningful only in the low-

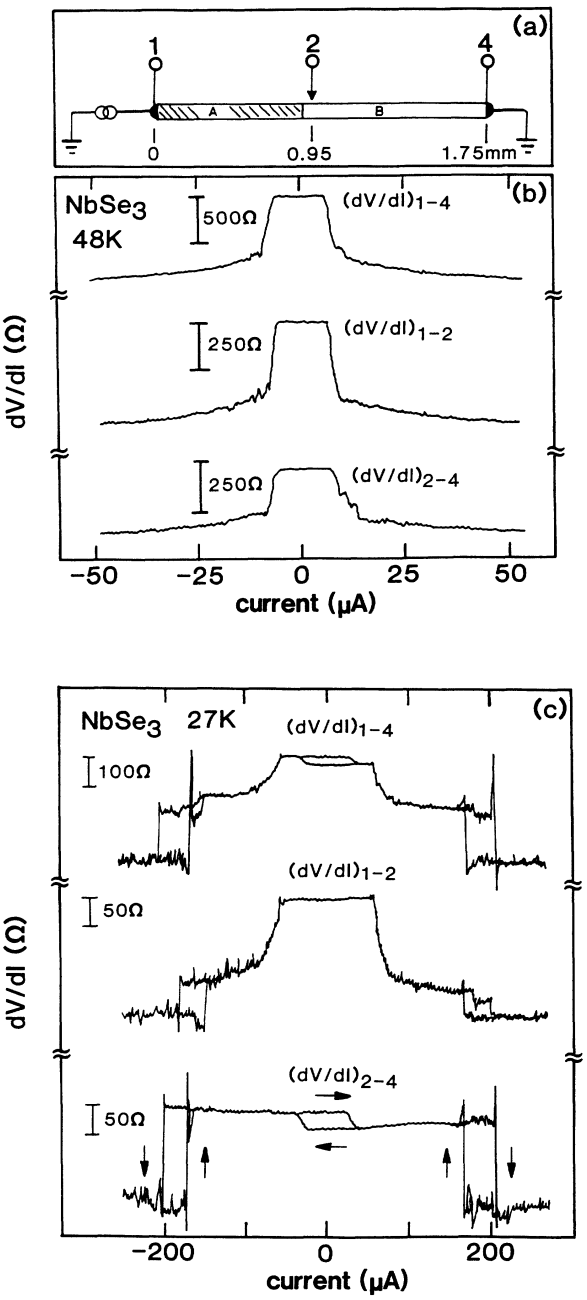

FIG. 12. (a) Three-terminal probe configuration for dV/dI measurements of Figs. 12(b) and 12(c), and Fig. 13. The regions "A" and "B" in the crystal become meaningful only at low temperatures, in the switching regime. (b) dV/dI traces for the entire $NbSe_3$ crystal (terminals 1 and 4), and left- and right-hand segments [see (a)], all measured at $T=48$ K. The CDW depins uniformly throughout the crystal at E_T at this temperature. (c) Same as (b), but for sample temperature $T=27$ K. Depinning is not uniform throughout the crystal. The top trace shows the dV/dI characteristics for the entire crystal. Strong low-field hysteresis is observed below E_T, and switching occurs at high bias current. The middle trace shows the dV/dI characteristics primarily for region A [see Fig. 12(a)]. No low-field hysteresis is observed in this "normally depinning" region. The bottom trace shows the dV/dI characteristics for region B [see Fig. 12(b)]. This region is associated with strong low-field hysteresis and switching.

temperature, switching regime.) Figure 12(b) shows dV/dI traces at 48 K corresponding to the crystal segments between probes 1 and 4, probes 1 and 2, and probes 2 and 4. At 48 K, the three regions depin simultaneously and display identical dV/dI characteristics. No hysteresis is present in the low-field resistance. This is not the case at lower temperatures that are within the switching regime.

Figure 12(c) shows localized dV/dI measurements of the same $NbSe_3$ crystal at 27 K. At this temperature the crystal consists of two well-defined regions A and B, which depin independently. These regions were mapped out in a series of I-V experiments similar to those described for Fig. 8. Region A depins normally at a current bias of 57 μA, whereas region B switches at a current bias roughly 3.5 times larger. The dV/dI plots of Fig. 12(c) were made with probe 3 raised and probe 2 placed inside region B. The top trace is the dV/dI response of the entire crystal, and the second and third traces correspond approximately to regions A and B. The second trace, measured mainly across region A, has a concave-upward shape characteristic of nonswitching CDW's except for a small contribution from region B. The third trace, measured across most of region B, has an entirely different shape. Excluding the region near zero bias, the trace resembles a hysteretic step function. The dynamic resistance of the switching region changes abruptly from the pinned, zero-field value to the saturated, high-field limit. The top trace, the response of the entire crystal, is a linear superposition of regions A and B.

Near zero bias, region B displays two repeatable and distinct resistivity states. The lower resistivity state is reached by increasing the current bias past $I_P = 33$ μA and then reducing the bias to zero. The upper resistivity state is reached by sweeping the bias below $-I_P = 33$ μA and then back to zero. The low-field resistivity of region B displays a "memory" of the polarity of the preceding bias sweep, provided that the bias exceeds either of the critical values $\pm I_P$. This polarization effect is large, approximately 15% of the low-field resistance of region B. The strong polarization effect is closely connected with switching since it occurs in the switching region of the crystal.

Figure 12(c) shows that the critical bias I_P, the polarization threshold for switching region B, is comparable to the threshold bias of nonswitching region A. This suggests that polarization in region B is caused by the CDW depinning from impurities in some parts of the region, but remaining pinned in others. CDW current in region B is prevented from flowing by the CDW elasticity, until region B switches (and completely depins) at a much higher bias. The temperature dependence of the polarization effect is consistent with this interpretation. Figure 13 shows dV/dI measurements across region B from 48 to 28 K. Between 48 and 40 K, the dV/dI curve loses its concave-upward shape past threshold, and low-field hysteresis sets in at the same time. A change of scale at 40 K and then at 35 K clarifies what is happening to the CDW in region B. As temperature is reduced, the CDW only partially depins at the higher temperature threshold I_T. Further depinning takes place past I_T, and by 37 K a

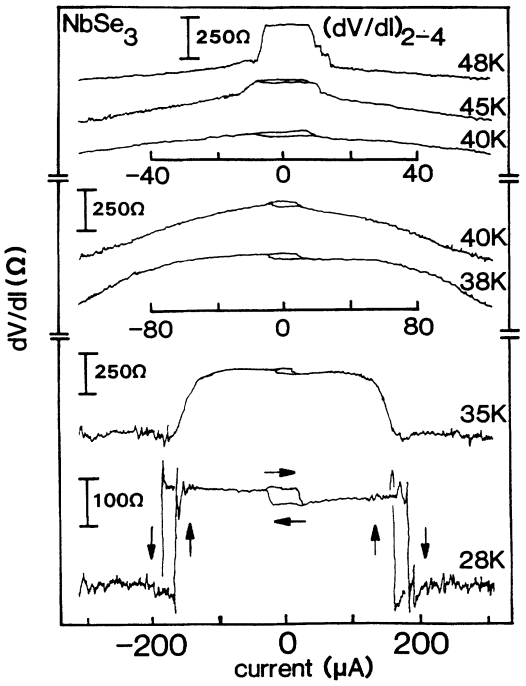

FIG. 13. dV/dI vs I at selected temperatures for the switching region (region B) of the $NbSe_3$ crystal of Fig. 12.

second threshold is clearly evident as a pronounced downward bend in the dV/dI curve. At lower temperatures, this bend sharpens into the switch that is observed at 28 K. The polarization field I_P is a remnant of the nonswitching threshold I_T at higher temperatures. Evidently, a large polarization and accompanying elastic strain is necessary to produce depinning at the switching threshold.

Near zero bias, the upper and lower resistivity states of region B appear to be just two of an infinite number of stable polarization configurations of the CDW. Figure 14 shows the low-field resistivity of region B in closer detail at 38 K. If current is monotonically swept from below $-I_P = -10$ μA to above $+I_P$ and then back again, only

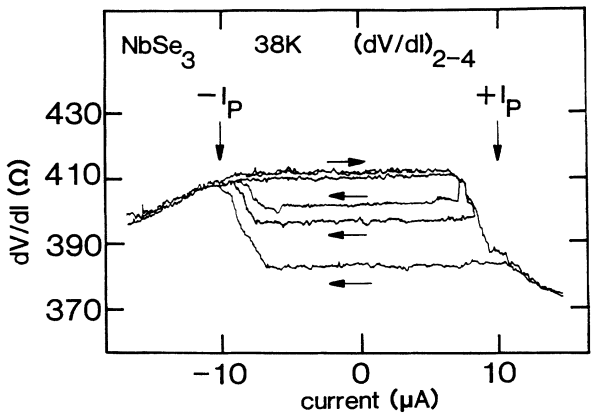

FIG. 14. Detail of low-field polarization states of the $NbSe_3$ crystal of Figs. 12 and 13. The arrows indicate bias-sweep direction.

the upper and lower resistivity states of region B are mapped out. If the current sweep is reversed as the transition is made from one state to the other, however, then a series of sublevels are attained inside the hysteresis loop. Two such sublevels are indicated in the figure.

Similar polarization and memory effects have been previously observed in $NbSe_3$ by Ong *et al.*, although they were not recognized as being associated with switching.[37] In general, polarization experiments have been performed using only a two-contact configuration, which can obscure inhomogeneous polarization and current distributions. Mihaly and Tessema[38] have also reported related polarization effects in $K_{0.3}MoO_3$, where switchinglike behavior is observed. The large magnitude of the effect that we observe here in switching $NbSe_3$ is due to the coexistence of switching and nonswitching regions within the same crystal. In switching crystals that contain no nonswitching regions, we have observed smaller polarization effects.

IV. ANALYSIS

A. Experimental implications

Switching in pure and iron-doped $NbSe_3$ is apparently caused by the same mechanism, although switching occurs at higher temperatures in Fe_xNbSe_3 than in $NbSe_3$. In both materials, measurements of differential resistance suggest that switching corresponds to an effective collapse of CDW pinning past threshold. Consequently, CDW's in switching crystals make an abrupt transition from a pinned, zero-velocity state to an effectively high-field state. This process of depinning is very different from the usual process of phase depinning that occurs in nonswitching crystals, as is underscored by the atypical temperature *in*dependence of switching critical fields E_c. Threshold fields are generally large in switching crystals, so that pinning forces must be large, but large threshold fields alone do not cause switching. Other attempts to distinguish switching from nonswitching crystals—by crystal quality and by crystal dimensions—have also been unsuccessful. Surface inspection of switching crystals shows that switching crystals are not physically damaged or otherwise different from nonswitching crystals. By elimination, strong impurities or internal lattice defects remain as likely causes of switching.

Other experiments point directly to a random, internal distribution of strong pinning centers—such as strong impurities or lattice defects—as the probable cause of switching. As demonstrated by examination of hysteresis loops or by measurement of local conductivity within a single crystal, a characteristic feature of switching crystals is the tendency to break into spatially distinct domains of uniform CDW current. These domains are separated by phase-slip centers which convert excess CDW current into normal electronic current via periodic collapse of the CDW amplitude. Narrow-band noise measurements and temperature-gradient experiments show that strong-pinning centers and amplitude fluctuations can exist even inside current domains. Nonuniform pinning produces a large amount of CDW phase polarization, with a threshold for the onset of polarization effects that is clearly a remnant of the usual phase-depinning process.

In the analysis that follows, we shall first discuss previously proposed models of switching. These models prove to be inconsistent with experiment. We therefore propose another mechanism for switching: phase slippage and CDW amplitude fluctuations.

B. Phase-dynamical model of switching

In $NbSe_3$ and Fe_xNbSe_3, switching is associated with hysteresis, bistability, negative differential resistance, and chaos. Similar phenomena have been observed in other systems, e.g., semiconductors under large electric fields. There, the effects are attributed to single-particle processes such as thermal runaway, impact ionization, or avalanche breakdown. None of these single-particle processes appears appropriate to $NbSe_3$ or Fe_xNbSe_3. Impact ionization and avalanche breakdown require fields of at least 1000 V/cm, whereas in $NbSe_3$, switching results from fields between 0.1 and 1 V/cm. Thermal runaway is ruled out because it requires a material's resistivity to decrease with increasing temperature; in pure and iron-doped $NbSe_3$, switching occurs only when $d\rho/dT > 0$.

A number of models have been proposed to account for various aspects of CDW switching. Joos and Murray[23] have proposed a domain coupling model; Janossy and Kriza[24] have suggested a CDW self-blocking mechanism; Hall *et al.*[19] have considered a single-degree-of-freedom model with inertia, and Wonneberger[25] has proposed a single-degree-of-freedom model with current noise. A common feature of these models is that they ascribe switching to CDW phase dynamics, and neglect or assign an insignificant role to amplitude fluctuations. The models often reproduce certain experimental results, but they cannot describe all the phenomena of CDW switching discussed in this report.

In the domain coupling model of Joos and Murray, a switching crystal is divided into an arrangement of otherwise unspecified domains. When an electric field exceeds the threshold for CDW depinning, each domain is assigned a certain probability for depinning, and once depinned, a domain can trigger neighboring domains to also depin, so that a depinning wave propagates along a crystal. This model reproduces the delay times observed in pulsed switching experiments,[9] but the physics behind domains and their intercouplings is unclear, as is why they should behave differently in switching versus nonswitching crystals. From a mathematical point of view, the description is a kinetic Ising model.

The simplified nature of the Joos-Murray model results in problematic I-V characteristics. A more serious difficulty is that the model requires no CDW current to flow in a switching crystal until the CDW has depinned in all portions of the crystal; this is inconsistent with our experiments, which demonstrate that current domains may depin independently within a given crystal. The usefulness of the Joos-Murray model is that it involves a domain configuration (as observed experimentally) with

tractable statistics in the time domain (an issue not discussed here). It is a many-degree-of-freedom model.

The CDW self-blocking model of Janossy and Kriza is also a many-degree-of-freedom model. It proposes that macroscopic polarization of a CDW interferes with depinning and delays CDW conduction until the CDW can relax from a polarized state. As discussed earlier, and illustrated in Figs. 13 and 14, large polarization effects are indeed associated with switching CDW's. In the self-blocking model, the origin of the unusual polarization (as opposed to polarization in nonswitching crystals) remains unspecified. An interesting implication of the model is that if dc bias is swept slowly enough, then switching should not be observed in the I-V characteristics of a crystal. In our experiments, however, we observe no unusual time dependence (at long time scales) in the switching characteristics of $NbSe_3$ or Fe_xNbSe_3. Finally, just as with the Joos-Murray model, the self-blocking model requires that no CDW current flows in a crystal until the CDW depins along the entire crystal length (which is inconcistent with experiment, as stated previously).

Both the CDW inertial model of Hall *et al.* and the CDW current model of Wonneberger *et al.* are based on the single-particle classical equation of motion proposed by Grüner, Zawadowski, and Chaikin,[21]

$$\frac{d^2x}{dt^2}+\frac{1}{\tau}\frac{dx}{dt}+\frac{\omega_0^2}{Q}\sin Qx=\frac{e}{m^*}E\ , \tag{2}$$

where x is the CDW center-of-mass coordinate, t is a time variable, τ is a time constant describing dissipation, ω_0 is a pinning frequency representing the strength of the impurity potential, m^* is the Fröhlich mass of the CDW electrons, and E is the applied electric field. Usually, the inertial term (first term on the left) is neglected because the phase relaxation rate (order 10^{-11} s) is much faster than either ω_0 or the frequency of the applied electric field. In the inertial model of switching, the first term in Eq. (2) is retained, which is equivalent to specifying that $\omega_0 \gtrsim 1/\tau$. Thus the inertial model requires either large pinning or small damping. In the current-noise model, the inertial term is neglected, but an additional noise term is added to the right-hand side of Eq. (2). The magnitude of the noise term is a function of the CDW velocity, so Eq. (2) must be solved self-consistently. For switching to occur, current noise must increase sharply as the CDW velocity approaches zero. The physical origin of this noise remains unspecified.

The inertial model of switching is equivalent to the resistively-shunted-junction (RSJ) model with capacitance, which is commonly discussed in the Josephson-junction literature.[39] It predicts switching, hysteresis, bistability, and chaos, all of which are observed in switching crystals of $NbSe_3$. However, the parameters of the model are not self-consistent when applied to CDW dynamics. The model requires either very large pinning (large values of ω_0) or very small damping (small values of $1/\tau$) for switching to occur, but neither assumption is justified by experiment. Typically, ω_0 in nonswitching crystals is much smaller than $1/\tau$, $\omega_0\tau \sim 3\times 10^{-2}$. The phase relaxation rate $1/\tau$ does not appear to change in switching crystals, because the high-field conductivity limit is the same for switching as for nonswitching crystals. Large pinning is observed in switching crystals, but it is not so large as to indicate underdamped motion. Since threshold fields[21] scale as ω_0^2, underdamped motion in $NbSe_3$ would imply threshold fields in switching crystals that are roughly 1000 times larger than those in nonswitching crystals. In $NbSe_3$ crystals, the ratio between switching and nonswitching threshold fields is between a factor of 3 and 10. This discrepancy can be overcome by invoking velocity-dependent pinning or damping, but such extensions appear inconsistent with ac-conductivity measurements.[18,26] Lastly, a serious limitation of the single-degree-of-freedom inertial model is that it is unable to provide a plausible explanation for the existence of current domains.

The current-noise model of Wonneberger suffers from the same problems with current domains. The most objectionable feature of this model, however, is the functional form of the conduction noise necessary to induce switching and hysteresis.[25] During measurements of current noise using a voltage-driven configuration, we have observed no large increases in noise near the critical switching field E_c. This lack of noise is inconsistent with the basic mechanism of Wonneberger's model.

C. A phase-slip mechanism for switching

A common limitation of all the models discussed above is a neglect of CDW amplitude fluctuations. Our experiments suggest that switching is intimately tied to the amplitude fluctuations that are associated with velocity discontinuities in switching crystals. The unusual phase polarization which precedes switching also suggests that a primary role is played by CDW pinning and pinning centers. In the next section, therefore, we turn to a discussion of how amplitude fluctuations can affect both the phase elasticity of a CDW and the effective pinning of a CDW at sites of especially strong pinning.

1. CDW elasticity and amplitude fluctuations

CDW dynamics can be drastically altered by amplitude fluctuations, because the CDW phase and amplitude are not exact normal coordinates of CDW motion.[2] Often this distinction is of little importance. If only weak impurities are present, then the CDW amplitude is uniform in the bulk of a crystal. Therefore the parameters which determine phase motion may be treated as constants. However, if CDW dynamics is dominated by phase slippage (as occurs in regions of CDW velocity discontinuity), rather than by the usual process of phase depinning, then amplitude fluctuations can result in an unstable CDW phase elasticity.

The elasticity of the CDW phase plays a critical role in CDW dynamics. In the Fukuyama-Lee-Rice (FLR) Hamiltonian,[3-5] the CDW phase responds as an elastic continuum to the net force resulting from impurity pinning and applied electric fields. The equilibrium phase $\phi(x)$ minimizes an energy given by

$$H=\int d^3x\left[\tfrac{1}{2}\sum_i K_i\left(\frac{d\phi}{dx_i}\right)^2 - \sum_i \rho_{\mathrm{CDW}} V_j \delta(\mathbf{x}-\mathbf{x}_j)\cos[\mathbf{Q}\cdot\mathbf{x}+\phi(\mathbf{x})] - e\rho_{\mathrm{eff}}\bar{\rho}E\phi(\mathbf{x})/Q\right] \quad (3)$$

where the first term represents the elastic energy of the CDW, the second term the pinning energy, and the third term the electric field energy. Here the K_i are elastic constants of the CDW phase, V_j is the strength of the jth impurity, and ρ_{eff} is the effective coupling of the CDW to the electric field E. The CDW elasticity is anisotropic. In directions transverse to the CDW wave vector $\mathbf{Q}$, the elastic constant is given by[5]

$$K_\perp=\eta^2 K \ , \quad (4)$$

where K is the longitudinal elastic constant and $\eta\sim 0.1$ is the bandwidth anisotropy of $NbSe_3$. Following Lee and Rice,[5] anisotropy may be formally eliminated by scaling the transverse spatial dimensions:

$$H_{\mathrm{elastic}}=\tfrac{1}{2}\int dx\int dy'\int dz'\,K'(\nabla'\phi)^2 \ , \quad (5)$$

where $dy'=dy/\eta$, $dz'=dz/\eta$, and $K'=\eta^2 K$.

The FLR Hamiltonian is inappropriate for describing large amounts of phase polarization, because it purposely neglects any fluctuations of the CDW amplitude. Since the CDW amplitude is determined by balancing the lattice energy cost of a Peierls distortion against the energy gained from enhanced electron-phonon interactions in a deformed lattice, large CDW phase gradients reduce the CDW amplitude for two reasons. First, deformations of the CDW phase require an amount of energy proportional to $(\nabla\phi)^2$, so the energy cost of a Peierls distortion is increased. Second, gradients of the CDW phase effectively change the CDW wave vector, so that the energy gained from electron-phonon interactions is reduced. For sufficiently large phase gradients, the CDW amplitude must collapse.

Large phase gradients also reduce the CDW phase elasticity. The general dependence of the restoring force $\delta H_{\mathrm{elastic}}/\delta\phi$ on $|\nabla\phi|$ is shown in Fig. 15. For small phase gradients, $\delta H_{\mathrm{elastic}}/\delta\phi$ is linear in $|\nabla\phi|$, as discussed by Fukuyama. For large phase gradients, the CDW amplitude collapses, the CDW phase becomes indeterminate, and therefore the restoring force $\delta H_{\mathrm{elastic}}/\delta\phi$ must vanish. The effective restoring force attains a maximum value at some critical phase gradient χ_c. For phase gradients larger than χ_c, the phase elasticity begins to decrease and the restoring force enters an unstable regime. In this regime, amplitude collapse occurs because of positive feedback between increasing polarization and decreasing elasticity.

When amplitude collapse is complete, the CDW phase slips by π (or a multiple, depending on boundary conditions), the gradient $|\nabla\phi|$ decreases, and the amplitude reforms. If polarization has built up over a long distance L, then the reduced gradient after collapse is $\chi_m-2\pi/L$,

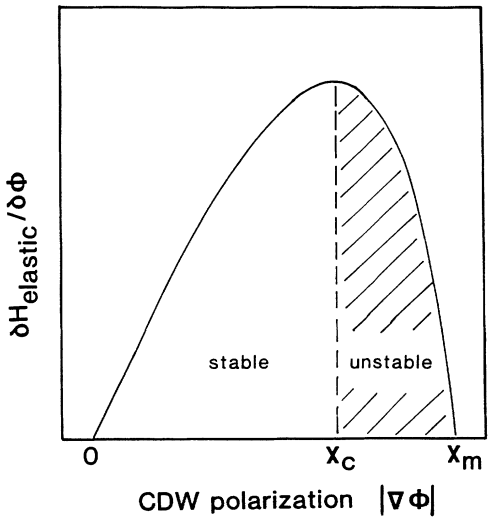

FIG. 15. CDW phase elasticity as a function of CDW phase polarization (see text).

where χ_m is the gradient at which the CDW amplitude vanishes. When $2\pi/L<\chi_m-\chi_c$, the CDW elasticity remains unstable after the amplitude reforms, and collapse reoccurs until the forces which produce polarization are reduced. In essence, the polarization $\chi_m-\chi_c$ defines a length scale for the stability of the phase mode. Large polarization of a CDW over distances longer than $2\pi/(\chi_m-\chi_c)$ can lead to an extremely nonlinear response, e.g., abrupt depinning. The critical length for nonlinear effects may be estimated as follows. The energy density $\frac{1}{2}K\chi_m^2$ is at least as large as the CDW condensation energy $n(0)\Delta_0^2$, where $n(0)$ is the Fermi-level density of states and Δ_0 is the equilibrium value of the CDW gap. If χ is defined to be the fractional polarization $(\chi_m-\chi_c)/\chi_m$, then the *critical polarization length scale* is

$$L_c\gtrsim\xi\left(\frac{2\pi}{\chi}\right)[K/2n(0)\Delta_0^2\xi^2]^{1/2} \ , \quad (6)$$

where ξ is the CDW amplitude coherence length and $K/2n(0)\Delta_0^2\xi^2=\pi^2/8$.

2. *Switching and velocity discontinuities*

We propose that switching results from the combined effect of elastic instability and phase slip at strong-pinning centers; i.e., at crystal defects that strongly pin the CDW phase. Later we will consider in detail the nature of the strong-pinning centers implied by our experiments, but for now we simply define a strong-pinning center as a defect whose pinning strength exceeds the elasticity of the CDW phase.[4,5] Depinning from a strong-pinning center therefore occurs only when the CDW amplitude collapses.

In order to make a connection with the results of Fig. 15, we first consider a highly simplified case in which a CDW is pinned by a concentration n_s of isolated strong-pinning centers in an otherwise perfect crystal at zero temperature. When an electric field is applied, segments

of the CDW that lay between pinning centers are restrained from sliding only by the elasticity of the CDW phase. As the strength of the electric field increases, these segments become increasingly polarized. Eventually, the increasing polarization shifts the CDW elasticity from the stable to the unstable region of Fig. 15. Phase slippage then occurs at the strong-pinning centers and the CDW begins to slide. If the spacing $L=(\eta^2 n_s)^{-1/3}$ of pinning sites is large enough, then the CDW polarization is not significantly relieved by the phase-slip process. Consequently, the CDW elasticity remains in the unstable regime of Fig. 15 and the CDW velocity is determined only by the applied electric field. The J-E curve is therefore linear past threshold and the CDW jumps immediately into the high-field conductivity state. This produces a sharp switch at threshold and a flat dV/dI curve past threshold. The J-E curve is also hysteretic, because the electric field must be reduced below a smaller threshold $E_T'=E_T(L_c/L)^2$ in order for the CDW elasticity to become stable again. Thus the instability of the CDW phase under large amounts of polarization provides a natural mechanism for abrupt depinning and hysteresis.

Besides abrupt depinning and hysteresis, phase slippage can also produce velocity discontinuities under certain conditions. It is known experimentally that not all strong-pinning centers produce velocity discontinuities, since temperature-gradient experiments demonstrate the existence of phase-slip centers within current domains. It is also expected theoretically that not all phase-slip centers, e.g., isolated strong impurities, will be strong enough to break the velocity coherence of a CDW. The problem of velocity discontinuities has been considered in some detail by Gorkov, and independently by Ong and Maki.[34] For a crystal of sufficient width, the most efficient means of creating a CDW velocity discontinuity is via phase vortices.[34] Around a phase vortex, the CDW phase is described by $\phi=\arctan(y/\eta x)$, where the z axis is chosen to be parallel to the vortex core. The energy density $\epsilon_{\rm break}$ necessary to create a phase vortex is quite large compared with the energy density sufficient to depin a CDW. For strong impurities, this ratio is

$$\epsilon_{\rm break}/\epsilon_{\rm depin}\sim(L_0/\xi)[1+\alpha\ln(L_0/\xi)]\ , \tag{7}$$

where the first term within the square brackets is due to the vortex core and the second term to the elastic energy of the CDW phase. The constant $\alpha=K/n(0)\Delta_0^2\xi^2$ is of order unity, and for strong impurities the FLR length L_0 is just the mean distance between impurities. For threshold fields less than 1 V/cm, the ratio L_0/ξ is greater than 8 [assuming $\Delta_0=35$ meV and $\xi=20$ Å (Ref. 40)]. Therefore the energy required to create a vortex is an order of magnitude larger than the energy required to depin a CDW. This implies that a random distribution of strong impurities will not lead to the velocity discontinuities that are associated with switching in $NbSe_3$. (A similar conclusion holds for weak impurities.)

We suggest that the strong-pinning and phase-slip centers associated with velocity discontinuities arise from "ultrastrong"-pinning sites. Essentially, ultrastrong-pinning centers are large-scale versions of single impurities. Ultrastrong-pinning centers, for example, might arise from abnormally high local concentrations of strong impurities, or other crystal defects such as dislocation lines of phase inclusions (in the case of Fe_xNbSe_3). Because of their larger size, however, ultrasong-pinning centers tend to form vortices and hence velocity discontinuities.

The pinning effect on an ultrastrong-pinning site depends on its size and, to a more limited degree, on its shape. When a center's cross section is one dimensional, amplitude collapse occurs over the entire center. The pinning energy of the center is

$$E(\zeta)\sim\eta n(0)\Delta_0^2\xi^2\zeta\ , \tag{8}$$

where ζ is the effective center diameter. In contrast, if a center's cross section is two dimensional, then amplitude collapse over the entire center is energetically unfavorable. Instead, phase slippage occurs by vortex rings that form around an effective circumference of the center. The pinning energy of the center would be roughly

$$E(\zeta)\sim\eta n(0)\Delta_0^2\xi^2\zeta[1+\alpha\ln(\zeta/\eta\xi)]\ , \tag{9}$$

where ζ now represents the effective circumference. For any shape center, the local energy density necessary for phase slippage is about

$$\epsilon(\zeta)\sim\eta E(\zeta)/\zeta^3\ . \tag{10}$$

Whenever the characteristic size of an ultrastrong-pinning center becomes comparable to the transverse dimensions of a crystal, the center is likely to cause a discontinuity in CDW current.

Large phase polarization, and thus switching, would be produced by a distribution of ultrastrong-pinning centers whose concentration is sparse on the length scale of $[K/2\epsilon(\zeta)]^{1/2}$ where ζ is the effective center size. When a crystal contains centers with a variety of sizes, the spatial arrangement of the centers as well as their sizes is important. With an absolutely uniform distribution of centers, two additional length scales are set by those centers whose combined size ζ_M and density $n(\zeta_M)$ have the largest pinning effect on the CDW:

$$n(\zeta_m)E(\zeta_M)=\max_{\zeta}\{n(\zeta)E(\zeta)\}\ . \tag{11}$$

The *phase-slip length scale* $L_{\rm PS}$ is the mean distance between defects of size ζ_M. The *switching length scale* $L_{\rm sw}$ is the critical pinning center spacing that determines whether depinning causes the CDW phase elasticity to enter the unstable regime of Fig. 15:

$$L_{\rm sw}\gtrsim[K/2\epsilon(\zeta_M)]^{1/2}\ . \tag{12}$$

In the absence of additional impurities, a CDW depins when the electric field energy density exceeds $n(\zeta_M)E(\zeta_M)$. Switching occurs if the phase-slip length scale is longer than the switching length scale.

Real switching crystals have pinning inhomogeneities that presumably correspond to a random distribution of centers, not a uniform distribution. Randomness complicates the definition of phase-slip and switching length scales. For a given electric field, whether phase slippage

occurs at centers of a particular size ζ depends not only on the product $n(\zeta)E(\zeta)$, but also on the size and density of neighboring centers. The dominant defect size ζ_M can be lowered by avalanche effects. If ζ_M is the dominant size in a uniform distribution, then in a random distribution some centers of size ζ_M will occur in portions of a crystal that have less pinning than the average. The CDW at those centers will depin at field energies less than $n(\zeta_M)E(\zeta_M)$. The premature depinning will increase the strain on neighboring sections that have not yet depinned, and the additional strain can trigger a depinning wave within the crystal. Avalanche events of this nature can explain the sublevels within hysteresis loops, the breakup of switches under temperature gradients, and the delay times observed in pulsed experiments. Avalanche events also provide an important connection with the concept of a depinning wave in the Joos-Murray model.

3. *Regimes of switching*

For clarity, our discussion has thus far neglected the complications caused by finite-temperature effects and the presence of weak impurities. In this section, we consider these effects, which play an important role in determining whether switching is observed in real crystals.

Impurity concentrations. When only weak impurities are present within a CDW conductor, their concentration determines a FLR phase-coherence length L_W.[3-5] When both weak- and strong-pinning centers are present, the ratio of the weak-impurity FLR length L_W to the phase-slip length L_{PS} determines the qualitative nature of CDW dynamics. For $L_{PS} \gg L_W$, CDW sliding is dominated by phase depinning, but for $L_{PS} \ll L_W$, CDW dynamics is governed by phase slip. For $L_{sw} \ll L_{PS} \ll L_W$, switching can occur. The existence of these regimes has at least two experimental implications. First, doping a crystal with strong impurities will cause switching only if the weak-impurity concentration is sufficiently low. If the weak-impurity concentration is too large, then L_W is comparable to L_{sw} and consequently the condition for switching cannot be satisfied. Second, the current contacts to a crystal, even though they may strongly pin a CDW, in general will not cause switching. In a crystal with only weak impurities, the phase-slip length is simply the distance between contacts. Since typical crystal lengths are much longer than the FLR length, contacts cannot cause switching. Even if a sample's length were reduced below the FLR length, switching still might occur, unless the weak-impurity concentration was sufficiently low so that $L_{sw} \ll L_W$. This might explain why simply reducing the length of nonswitching samples has not been observed to induce switching.

Finite-temperature effects. Nonzero temperatures cause the phase-slip and switching lengths to change from their $T=0$ values. In superfluids[41] and superconductors,[42] phase slippage is thermally activated. Gill[43] has recently proposed that phase slippage at the contacts of CDW conductors is also thermally activated. The activation energy in Gill's work would correspond to the defect energy $E(\zeta)$ described in this paper. The result of thermal activation would be to reduce the pinning effect of small centers compared to the effect of large centers. For uniform distributions, this would make both the dominant center size ζ_M and the switching threshold field strong functions of temperature.

The fact that switching thresholds are independent of temperature is evidence that strong pinning centers are distributed *non*uniformly. If depinning occurs by phase-slip cascades, then switching critical fields should be strongly temperature dependent only until the dominant centers are "frozen in"; after that, threshold fields should be determined by the spatial arrangement of the dominant centers. In $NbSe_3$, thermal activation is consistent with the rapid increase in threshold field that is associated with the onset of switching. Figure 16 shows the threshold field as a function of temperature for a switching $NbSe_3$ crystal. Switching occurs below 40 K, where the threshold field is relatively independent of temperature. Above 40 K, the threshold field has been fitted to

$$E_T(T)=E_0\exp[E(\zeta)/k_BT] , \tag{13}$$

where $E_0=7.0$ μV/cm, $E(\zeta)=41$ meV, and k_B is Boltzmann's constant. The value of $E(\zeta)$ is relatively insensitive to the form assumed for $E_T(T)$; a fit to $E_T(T)=(k_BT/L')\exp[E(\zeta)/k_BT]$ yields $E(\zeta)=50$ meV. Assuming that Eq. (8) applies, 40 meV corresponds to $\zeta=0.1$ μm. Below 40 K, the sharp change in slope indicates that thermal activation is no longer important.

Thermal activation during the onset of switching also agrees qualitatively with the consistent decrease in switching onset temperatures that coincides with increasing crystal quality. In general, one would expect that smaller ultrastrong-pinning centers would be necessary to induce switching in higher-quality crystals, since the effect of weak impurities is smaller in these crystals. Therefore, higher-quality crystals should have lower switching onset temperatures. This correlation is indeed observed in our experiments and in the experiments of other groups. Switchinglike behavior occurs at very low temperatures in extremely-high-quality $NbSe_3$ crystals. Coleman[30] has reported striking zero-differential resistance anomalies at 1.1 K in $NbSe_3$ crystals that have

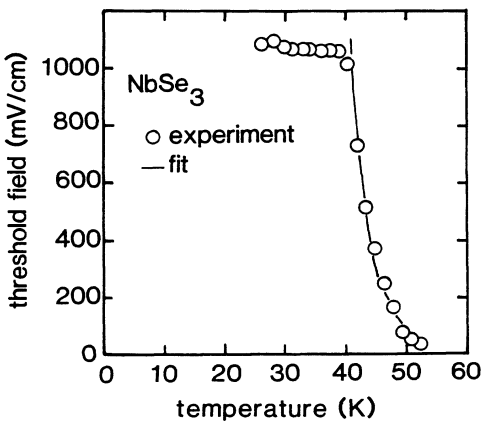

FIG. 16. Fit of the onset of switching in $NbSe_3$ to an activated temperature behavior. The solid line is Eq. (13), with parameters given in the text.

threshold fields of ~ 1 mV/cm at 48 K. Switching occurs at the next lowest temperatures (~ 30 K) in the moderate-quality $NbSe_3$ used in the present experiments ($E_T \sim 30$ mV/cm at 48 K). Switching occurs at the highest temperatures (~ 50 K) in Fe_xNbSe_3, which even in nonswitching crystals has threshold fields of at least 100 mV/cm at 48 K.

V. CONCLUSION

Switching is a fascinating and apparently rather general feature of CDW dynamics. It is the first transport phenomenon in which amplitude dynamics is as important as phase dynamics to a description of CDW motion. Our experiments have demonstrated the important relationship between phase polarization, strong pinning, and phase slip in the switching process.

The occurrence of switching in nominally pure $NbSe_3$, as well as Fe_xNbSe_3, suggests that strong-pinning centers may result not only from strong impurities, but also lattice defects. Gross lattice defects—such as grain boundaries or twinning—are probably unimportant. Grain boundaries and twinning occur infrequently in $NbSe_3$ crystals,[44] at levels of less than once in 100 μm^3; such levels are too low to explain the nonuniform pinning that is observed in temperature-gradient experiments. On the other hand, smaller defects—such as dislocation lines—could strongly pin a CDW at densities low enough to give large variations in pinning. For example, a dislocation-line density of 4 μm^{-3} with an average line length of 0.25 μm (corresponding to a dislocation density of 1 μm^{-2}) would lead to $\pm 50\%$ pinning-energy fluctuations between 1 μm^3 segments in $NbSe_3$. Roughly order-of-magnitude pinning fluctuations would be relatively common, and $\pm 50\%$ variations would persist over distances of 100 μm (assuming a 1-μm^2 crystal cross section).

Little has been published about defect densities in $NbSe_3$. Satellite dark-field micrographs of some $NbSe_3$ crystals show lattice dislocation densities of roughly 1 μm^{-2}, while other crystals are apparently defect free.[45] The conventional method of sample growth of $NbSe_3$ and Fe_3NbSe_3 should lead to vacancy densities of about 10 ppm, and vacancies are known to precipitate dislocations. The observed "aging" effect of switching crystals may be due to physical or chemical changes around dislocation sites. Etches of H_2SO_4 preferentially attack dislocation sites in niobium,[46] and they may preferentially attack dislocations in $NbSe_3$. This might explain why H_2SO_4 would restore switching in aged batches, but not induce switching in originally nonswitching crystals, as observed. It would be highly desirable to examine the strong-pinning centers of our switching crystals by transmission electron microscopy.

Finally, we note that many of the ideas expressed here for $NbSe_3$ and Fe_xNbSe_3 should be applicable to other sliding CDW systems, for example, $K_{0.3}MoO_3$, TaS_3, and $(NbSe_4)_{3.33}I$. Experiments on these compounds, analogous to the experiments reported here, will be of importance in the development of a complete model of CDW switching.

ACKNOWLEDGMENTS

We thank R. V. Coleman, S. Coppersmith, S. Doniach, L. M. Falicov, M. Inui, A. Janossy, B. Joos, and M. S. Sherwin for useful discussions and interactions. This work was supported by National Science Foundation Grant No. DMR-84-00041. One of us (A.Z.) also acknowledges support from the Alfred P. Sloan Foundation.

*Present address: AT&T Bell Laboratories, Murray Hill, NJ 07974-2070.

[1]For a review, see G. Grüner and A. Zettl, Phys. Rep. **119**, 117 (1985).
[2]P. A. Lee, T. M. Rice, and P. W. Anderson, Solid State Commun. **14**, 703 (1974).
[3]H. Fukuyama, J. Phys. Soc. Jpn. **41**, 513 (1976).
[4]H. Fukuyama and P. A. Lee, Phys. Rev. B **17**, 535 (1978).
[5]P. A. Lee and T. M. Rice, Phys. Rev. B **19**, 3970 (1979).
[6]R. M. Fleming and C. C. Grimes, Phys. Rev. Lett. **42**, 1423 (1979); R. M. Fleming, Phys. Rev. B **22**, 5606 (1980).
[7]N. P. Ong and P. Monceau, Phys. Rev. B **16**, 3443 (1977).
[8]P. Monceau, N. P. Ong, A. M. Portis, A. Meerschaut, and J. Rouxel, Phys. Rev. Lett. **37**, 602 (1976).
[9]A. Zettl and G. Gruner, Phys. Rev. B **26**, 2298 (1982).
[10]R. P. Hall and A. Zettl, Solid State Commun. **50**, 813 (1984).
[11]M. P. Everson and R. V. Coleman, Phys. Rev. B **28**, 6659 (1984).
[12]G. Kriza, A. Janossy, and G. Mihaly, in *Charge Density Waves in Solids*, edited by Gy. Hutiray and J. Sólyom (Springer, New York, 1985), p. 426.
[13]L. Mihaly and G. Grüner, Solid State Commun. **50**, 807 (1984).
[14]Z. Z. Wang, P. Monceau, M. Renard, P. Gressier, L. Guemas, and A. Meerschaut, Solid State Commun. **47**, 439 (1983).
[15]J. Dumas, C. Schlenker, J. Marcus, and R. Buder, Phys. Rev. Lett. **50**, 757 (1983); J. Dumas and C. Schlenker, in Ref. 12, p. 439.
[16]H. Mutka, S. Bouffard, J. Dumas, and C. Schlenker, J. Phys. (Paris) Lett. **45**, L729 (1985).
[17]R. P. Hall, M. S. Sherwin, and A. Zettl, Phys. Rev. Lett. **52**, 2293 (1984).
[18]R. P. Hall and A. Zettl, Solid State Commun. **55**, 307 (1985).
[19]R. P. Hall, M. Sherwin, and A. Zettl, Phys. Rev. B **29**, 7076 (1984).
[20]J. Bardeen, Phys. Rev. Lett. **42**, 1498 (1979); **55**, 1010 (1985).
[21]G. Grüner, A. Zawadowski, and P. M. Chaikin, Phys. Rev. Lett. **46**, 511 (1981).
[22]Leigh Sneddon, M. C. Cross, and Daniel S. Fisher, Phys. Rev. Lett. **49**, 292 (1982).
[23]B. Joos and D. Murray, Phys. Rev. B **29**, 1094 (1984).
[24]A. Janossy, G. Mihaly, and L. Mihaly, in Ref. 12, p. 412.
[25]W. Wonneberger and H. J. Breymayer, Z. Phys. B **56**, 241 (1984).

[26]R. P. Hall and A. Zettl, following paper, Phys. Rev. B **38**, 13 019 (1988).
[27]M. S. Sherwin, R. P. Hall, and A. Zettl, this issue, Phys. Rev. B **38**, 13 028 (1988).
[28]M. Inui, R. P. Hall, S. Doniach, and A. Zettl, this issue, Phys. Rev. B **38**, 13 047 (1988).
[29]R. P. Hall, M. F. Hundley, and A. Zettl, Phys. Rev. Lett. **56**, 2399 (1986).
[30]R. V. Coleman, Synth. Met. **19**, 795 (1987).
[31]P. B. Littlewood, Phys. Rev. B **33**, 6694 (1986).
[32]W. J. Skocpol, M. R. Beasley, and M. Tinkham, J. Low. Temp. Phys. **16**, 145 (1974).
[33]P. W. Anderson, Rev. Mod. Phys. **38**, 298 (1966).
[34]Phase slippage at current-injection contacts has been discussed previously. See N. P. Ong, G. Verma, and K. Maki, Phys. Rev. Lett. **52**, 663 (1984); N. P. Ong and Kazumi Maki, Phys. Rev. B **32**, 6582 (1985); L. P. Gor'kov Pis'ma Zh. Eksp. Teor. Fiz. **38**, 76 (1983) [JETP Lett. **38**, 87 (1983)]; I. Batistic, A. Bjelis, and L. P. Gor'kov, J. Phys. (Paris) Colloq. **45**, 1049 (1984).
[35]R. P. Hall and A. Zettl, Solid State Commun. **57**, 27 (1986).
[36]M. F. Hundley and A. Zettl, Phys. Rev. B **33**, 2883 (1986); S. E. Brown, A. Janossy, and G. Grüner, *ibid.* **31**, 6869 (1985); X. J. Zhang and N. P. Ong, *ibid.* **30**, 7343 (1984); J. W. Lyding, J. S. Hubacek, G. Gammie, and R. E. Thorne, *ibid.* **33**, 4341 (1986).
[37]N. P. Ong, D. D. Dugan, C. B. Kalem, and T. W. Jing, in Ref. 11, p. 387.
[38]L. Mihaly and G. X. Tessema, Phys. Rev. B **33**, 5858 (1986).
[39]D. E. McCumber, J. Appl. Phys. **39**, 3113 (1968); W. C. Stewart, Appl. Phys. Lett. **12**, 277 (1968); P. Lindelof, Rep. Prog. Phys. **44**, 949 (1981).
[40]A. Fournel, J. P. Sorbier, M. Konczykowski, and P. Monceau, Phys. Rev. Lett. **57**, 2199 (1986).
[41]J. S. Langer and M. E. Fisher, Phys. Rev. Lett. **19**, 560 (1967).
[42]M. Tinkham, *Introduction to Superconductivity* (McGraw-Hill, New York, 1975).
[43]J. C. Gill, Physica **143B**, 49 (1986).
[44]J. L. Hodeau, M. Marezio, C. Roucau, R. Ayroles, A. Meerschaut, J. Rouxel, and P. Monceau, J. Phys. C **11**, 4117 (1978).
[45]C. H. Chen, R. M. Fleming, and P. M. Petroff, Phys. Rev. B **27**, 4459 (1983).
[46]S. Amelinckx, *Direct Observation of Dislocations* (Academic, New York, 1964).

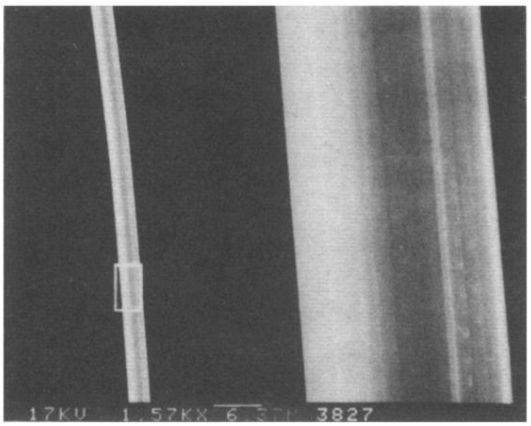

FIG. 4. Scanning-electron-microscopy micrograph of a switching $NbSe_3$ crystal. No surface defects are apparent. Left: typical crystal section. Right: detail of boxed region on the left, magnification by an additional factor of 10. Scale bar of 6.37 μm refers to the left-hand photo.